



Fuzzy neural network and observer-based fault-tolerant adaptive nonlinear control of uncertain 5-DOF upper-limb exoskeleton robot for passive rehabilitation

Baraka Olivier Mushage · Jean Chamberlain Chedjou · Kyandoghere Kyamakya

Received: 31 May 2016 / Accepted: 27 October 2016 / Published online: 4 November 2016
© Springer Science+Business Media Dordrecht 2016

Abstract This paper investigates the control of a 5-DOF upper-limb exoskeleton robot used for passive rehabilitation therapy. The robot is subject to uncertain dynamics, disturbance torques, unavailable full-state measurement, and different types of actuation faults. An adaptive nonlinear control scheme, which uses a new reaching law-based sliding mode control strategy, is proposed. This scheme incorporates a high-gain state observer with dynamic high-gain matrix and a fuzzy neural network (FNN) for state vector and nonlinear dynamics estimation, respectively. Using dynamic parameters, the scheme provides an efficient mean for simultaneously tackling the effects of FNN approximation errors, disturbance torques and actuation faults without any prior bounds knowledge and fault detection and diagnosis components. Using simulation results, it is shown that with the presented scheme, faster response, fewer oscillations during transient phase, good tracking accuracy, and chattering-free control torques with lower amplitudes are obtained.

Keywords Actuation fault · Adaptive nonlinear control · Upper-limb exoskeleton · Fuzzy neural network · High-gain state observer

1 Introduction

Thanks to some important advances in the research for efficient and safe control strategies of electromechanical and robotic devices, upper-limb exoskeletons are used for assisted rehabilitation therapy to provide passive arm movements such as the subject's limb can be moved following a given trajectory [1–9]. In particular, the 5-DOF upper-limb exoskeleton robot is able to assist with the shoulder, elbow and wrist joint movements [1,2]. Applied for assisted rehabilitation tasks, the repeatability, precision, control, and accuracy in the movements of an exoskeleton are very important for offering thorough and safe rehabilitation routines [10]. Therefore, controller design for such system is an important task.

Controller design can be problematic because of challenges related to real-world applications such as uncertain dynamics, external disturbances and unavailable full-state measurement. Knowing that these issues can affect the closed-loop system stability and/or performances, many approaches have been proposed for tackling them. For instance, for tackling the uncertainty problem, it has been proved that using adaptive controllers incorporating fuzzy logic systems for nonlinear dynamics approximation can provide very satisfactory results (see, for instance, in [11–15] and references therein). In order to deal with the actuation fault issue, a particular class of adaptive controllers known as fault-tolerant controllers (FTC) has been studied and successfully applied (see, for instance,

B. O. Mushage (✉) · J. C. Chedjou · K. Kyamakya
Institute of Smart Systems Technologies, University of
Klagenfurt, Klagenfurt, Austria
e-mail: olivermush@yahoo.fr

in [11, 14, 16–18] and references therein). These FTCs can use either some robust control approaches (passive FTC) [11, 14] or some fault detection and diagnosis (FDD) components (active FTC) [16–19] for dealing with actuation faults. For dealing with the unavailable full-state issue, especially when the system's dynamics is unknown, some model-free state observers such as fuzzy state observers [12, 14] or fuzzy sliding mode state observers [20] or high-gain linear state observers [13, 21, 22] are generally incorporated in the adaptive control scheme. These adaptive controllers are generally designed using some well-known nonlinear control techniques or strategies such as the sliding mode control (SMC) [23–28], feedback control [13, 21], the backstepping technique [11, 12, 14, 29, 30], and dynamic surface control [15]. Particularly for upper-limb exoskeleton robot control for passive rehabilitation, several works have been published showing good results obtained by applying different nonlinear control strategies such as the SMC [20, 23, 24, 31–34], feedback control [1, 2], fuzzy logic control [35, 36], impedance control [37], and passivity-based control [9]. For instance, an output feedback controller for a 5-DOF upper-limb exoskeleton robot was proposed in [1]. The proposed controller was designed such that it can provide good tracking performances despite uncertainties and disturbance torques. This controller uses an adaptive nonlinear state observer that provides estimation of velocity having only position information from sensors. An adaptive logic-based switching algorithm was proposed for the controller's parameters online adjustment. A robot system able to guide patient's wrist to move along planned linear or circular trajectories has been proposed in [35]. A hybrid position/force controller incorporating fuzzy logic was developed for that robot. The position controller was obtained as the fuzzy logic system output using the center-of-gravity method. The force controller was proposed as a combination of a conventional PI controller and a fuzzy PI tuner. The purpose of this late is the compensation of the joint friction of the robot and the unknown disturbing force from the subject/patient. A control system for a 3-DOF upper-limb rehabilitation and training robot was proposed in [36]. The presented system was based on a hierarchical structure that allows the execution of sequence of switching control laws for position, force, and impedance, corresponding to a given required training configuration. This system is a model-based nonlinear controller that requires

the knowledge of the robot's kinematics and dynamics for ensuring haptic transparency and patient safety. Therefore, identification of robot dynamics was performed using a maximum-likelihood type estimation [38]. Many works addressing the control of exoskeleton robots have used the SMC strategy for its robustness with respect to uncertainty and external disturbances (see, for instance, in [23, 24, 33, 39, 40]). However, it is known that the main drawback of SMC is the chattering phenomenon [20, 23, 24, 31–34, 40–42]. This phenomenon generates vibrations to the mechanical structure that could cause premature wear, or breaking of mechanical components. Thus, it is practically impossible to use conventional SMC with exoskeleton robots for the patients' safety. An approach for dealing with this issue was proposed in [40] for a 7-DOF exoskeleton robot arm. In this work, a chattering-free reaching law-based SMC combining the concept of the saturation function [43] and an exponential reaching law [44] was presented. However, to the best of our knowledge, a few has been done to propose approaches for nonlinear fault-tolerant adaptive control for upper-limb exoskeleton robotic systems, while these late can be subject to actuators faults. In fact, it has been reported that robot can be exposed to different types of faults such as total failure, partial fault, and bias fault [2, 16, 17, 45, 46]. Thus, designing controllers able to efficiently tackle actuators' faults may considerably increase patients' safety. However, such controller for a 5-DOF upper-limb exoskeleton robot has been studied in [2] but with only the actuators' loss of effective fault considered. Furthermore, actuation torque generated by this controller for meeting the control objective seems relatively too high, which is not energy efficient. Therefore, for a safe and efficient control of upper-limb exoskeleton robots, there is still a need for some improvements in terms of control energy, tracking performances, and robustness with respect to different types of faults.

Motivated by the above discussion and observations, this paper proposes a new adaptive nonlinear FTC scheme for the 5-DOF upper-limb exoskeleton robot presented in [1, 2, 47]. The study considers multiple challenges such as unavailable full system state information, uncertain nonlinear dynamics, disturbance torques, actuation faults (especially loss of effectiveness or gain faults, bias faults or the two considered simultaneously), and the need for faster response and improved tracking accuracy with relatively low amplitude control torques. For dealing with

the unavailability of full-state measurement and exact system's dynamics, the scheme incorporates a model-free high-gain state observer with a dynamic high-gain matrix for obtaining information about links' velocities, and a fuzzy neural network (FNN) for approximating the robot's unknown dynamics. To address the problem of control performance improvement and energy efficiency, a modified reaching law-based SMC is proposed, which has the particularity of providing a chattering-free control signal that ensures good tracking performances. The main advantages of the scheme introduced in this paper are as follows:

- (a) ability to efficiently and simultaneously tackle issues such as uncertain dynamics, torque disturbances, unavailable full state measurement and actuation faults of different types (unlike other schemes for exoskeletons robot control [1, 2, 9, 23, 24, 31–33, 35–37, 39, 40]);
- (b) chattering-free control signals without using some chattering avoidance methods that have been reported to alter the controllers' robustness feature [48] and that may involve some additional design parameters [20, 34, 40, 41, 43, 48–54];
- (c) alleviated online computation burden thanks to the use of the linear high-gain observer and to the fact that the FNN is used for approximating only one nonlinear vector function, unlike in [21, 55] where two nonlinear matrix functions have to be approximated;
- (d) unlike in other works involving FNN for robot control (see, for instance, in [20, 21, 24, 34, 41, 56, 57]), FNN approximation errors are compensated using dynamic parameters such that no prior error bound knowledge is required;
- (e) compensation of torque disturbances and actuation fault effects without any prior knowledge of any bound or any use of FDD devices as it is with many adaptive and FTC schemes [2, 16–19, 34, 44, 46];
- (f) convergence of the state observer and asymptotic stability of the closed-loop system are achieved using the proposed scheme and the update rules for the controller's dynamic parameters;
- (g) continuous and lower amplitudes control torques, shorter settling time, fewer oscillations, better tracking accuracy, or improved robustness.

The aforementioned effectiveness of the proposed approach is illustrated by simulating the controlled 5-DOF upper-limb exoskeleton robot in MATLAB. The

obtained results are compared to those obtained using the adaptive nonlinear FTC proposed in [2] for the same system.

The rest of this paper is organized as follows: In Sect. 2, we present the model of a 5-DOF upper-limb exoskeleton robot and state the control problem along with some preliminaries. In Sect. 3, the main results of this paper are developed, specifically the design of a high-gain state observer and a FNN-based adaptive fault-tolerant nonlinear controller for the robot. In Sect. 4, the 5-DOF upper-limb exoskeleton robot controlled by the designed adaptive fault-tolerant nonlinear controller is simulated in MATLAB. Section 5 is devoted to some concluding remarks.

2 Preliminaries and problem statement

In the mathematical developments presented throughout this paper, standard notations are used. \mathbb{R} represents the set of real numbers; \mathbb{R}^+ represents the set of positive real numbers; \mathbb{R}^n stands for the n -dimensional real vector space; $\mathbb{R}^{n \times n}$ denotes the $n \times n$ real matrix space. Let I_n be the column vector of n ones. The norm of vector $\mathbf{x} \in \mathbb{R}^n$ and that of matrix $\mathbf{A} \in \mathbb{R}^n$ are defined as $\|\mathbf{x}\| = \sqrt{\mathbf{x}^T \mathbf{x}}$ and $\|\mathbf{A}\|^2 = \text{tr} [\mathbf{A}^T \mathbf{A}]$, respectively. If y is scalar, then $|y|$ denotes its absolute value.

This section presents the dynamic equation of the 5-DOF upper-limb exoskeleton robot and its control problem. Some preliminaries are provided for a better understanding of the design of the controller proposed in this work, which involves the following steps:

- Step 1* Design of a state observer by specifying its parameters for good convergence properties;
- Step 2* Design of a nonlinear dynamics approximator: a FNN with its membership function, inputs, update rules and design parameters;
- Step 3* Design of a sliding function and a reaching law defining its dynamics;
- Step 4* Design of the fault-tolerant adaptive nonlinear controller and its parameters.

These preliminaries are provided through the presentation of the controller design for an ideal case corresponding to known system dynamics and available full-state measurement.

2.1 Exoskeleton control problem

The system to be controlled in this paper is the upper-limb exoskeleton robot that can simulate the most important 5-DOF in the human upper-limb movements that are: shoulder abduction/adduction, shoulder flexion/extension, the elbow flexion/extension, wrist flexion/extension, and internal/external rotation. This robot is modeled as a set of highly nonlinear coupled differential equations given as follows (the independent variable t is omitted for simplicity in notations) [1, 2, 47]:

$$\mathbf{M}(\mathbf{q})\ddot{\mathbf{q}} + \mathbf{C}(\mathbf{q}, \dot{\mathbf{q}})\dot{\mathbf{q}} + \mathbf{G}(\mathbf{q}) + \tau_d(\dot{\mathbf{q}}) = \tau \quad (1)$$

where $\mathbf{q}, \dot{\mathbf{q}}, \ddot{\mathbf{q}} \in \mathbb{R}^5$ are the position, velocity, and acceleration vectors, respectively; $\tau_d(\dot{\mathbf{q}}) \in \mathbb{R}^5$ is the disturbance torque vector, and $\tau \in \mathbb{R}^5$ is the joints actuation torque vector. $\mathbf{M}(\mathbf{q}) \in \mathbb{R}^{5 \times 5}$ is the generalized inertia matrix given by

$$\mathbf{M}(\mathbf{q}) = \begin{bmatrix} M_{11} & M_{12} & M_{13} & 0 & 0 \\ M_{21} & M_{22} & M_{23} & 0 & 0 \\ M_{31} & M_{32} & M_{33} & 0 & M_{35} \\ 0 & 0 & 0 & M_{44} & 0 \\ 0 & 0 & M_{53} & 0 & M_{55} \end{bmatrix}$$

where

$$\begin{aligned} M_{11} = & I_6 \sin(q_2) \cos(q_2) + I_4 \sin^2(q_2 + q_3) \\ & + I_5 \sin(q_2 + q_3) \cos(q_2 + q_3) + 2 \\ & + I_7 \sin^2(q_2 + q_3) + I_8 \cos(q_2) \sin(q_2 + q_3) \\ & + I_9 \cos(q_2) \cos(q_2 + q_3) + I_{10} \sin^2(q_2 + q_3) \\ & + I_{11} \cos(q_2) \sin(q_2 + q_3) + I_3 \cos^2(q_2) \\ & + I_2 + I_{19} + I_{12} \sin(q_2 + q_3) \cos(q_2 + q_3) \quad (2) \end{aligned}$$

$$\begin{aligned} M_{12} = M_{21} = & I_{13} \sin(q_2) + (I_{14} - I_{17}) \cos(q_2 + q_3) \\ & + I_{16} \sin(q_2 + q_3) + I_{15} \cos(q_2) \quad (3) \end{aligned}$$

$$\begin{aligned} M_{13} = M_{31} = & I_{14} \cos(q_2 + q_3) + I_{16} \sin(q_2 + q_3) \\ & - I_{17} \cos(q_2 + q_3) \quad (4) \end{aligned}$$

$$\begin{aligned} M_{22} = M_{18} = & I_{19} + I_{20} + I_9 \cos(q_2) \\ & + I_{10} + (I_{11} + 2I_8) \sin(q_3) \quad (5) \end{aligned}$$

$$\begin{aligned} M_{23} = M_{32} = & I_8 \sin(q_3) + I_{20} + I_9 \cos(q_3) \\ & + I_{11} \sin(q_3) + 2I_{10} \quad (6) \end{aligned}$$

$$M_{33} = I_{13} + I_{20} + 2I_{10} \quad (7)$$

$$M_{35} = M_{53} = I_{10} + I_{21} \quad (8)$$

$$M_{44} = I_{22} + I_{23} \quad (9)$$

$$M_{55} = I_{24} + I_{21} \quad (10)$$

and the carioles/centripetal matrix $\mathbf{C}(\mathbf{q}, \dot{\mathbf{q}}) \in \mathbb{R}^{5 \times 5}$ is given by

$$\mathbf{C}(\mathbf{q}, \dot{\mathbf{q}}) = \begin{bmatrix} C_1 \dot{q}_2 & C_2 \dot{q}_3 + C_3 \dot{q}_2 & C_4 \dot{q}_2 + C_5 \dot{q}_3 & 0 & 0 \\ C_6 \dot{q}_1 & C_7 \dot{q}_3 & C_8 \dot{q}_3 & 0 & 0 \\ C_5 \dot{q}_1 & C_9 \dot{q}_2 & 0 & 0 & 0 \\ C_{10} \dot{q}_2 & 0 & C_{11} \dot{q}_1 & 0 & 0 \\ 0 & C_{12} \dot{q}_2 & 0 & 0 & 0 \end{bmatrix}$$

where

$$\begin{aligned} C_1 = & 2[-I_3 \sin(q_2) \cos(q_2) + I_8 \cos(2q_2 + q_3) \\ & + I_4 \sin(q_2 + q_3) \cos(q_2) - I_9 \sin(2q_2 + q_3) \\ & - 2I_{10} \sin(q_2 + q_3) + I_{11} \cos(2q_2 + q_3) \\ & + I_7 \sin(q_2 + q_3) \cos(q_2 q_3) \\ & + I_{12}(1 - 2 \sin^2(q_2 + q_3))] \\ & + I_5 (1 - 2 \sin(q_2 + q_3) + I_6 (1 - 2 \sin^2(q_2))) \quad (11) \end{aligned}$$

$$\begin{aligned} C_2 = & 2[-I_{14} \sin(q_2 + q_3) + I_{16} \cos(q_2 + q_3) \\ & + I_{17} \sin(q_2 + q_3)] \quad (12) \end{aligned}$$

$$\begin{aligned} C_3 = & I_{13} \cos(q_2) - I_{14} \sin(q_2 + q_3) - I_{15} \sin(q_2) \\ & + I_{16} \cos(q_2 + q_3) + I_{17} \sin(q_2 + q_3) \quad (13) \end{aligned}$$

$$\begin{aligned} C_4 = & 2[I_8 \cos(q_2) \cos(q_2 + q_3) \\ & + I_4 \sin(q_2 + q_3) \cos(q_2 + q_3) \\ & - I_9 \cos(q_2) \sin(2q_2) \\ & + 2I_{10} \sin(q_2 + q_3) \cos(q_2 + q_3) \\ & + I_{11} \cos(q_2) \cos(q_2 + q_3) \\ & + I_7 \sin(q_2 + q_3) \cos(q_2 + q_3) \\ & + I_{12}(1 - 2 \sin^2(q_2 + q_3))] \\ & + I_5 (1 - 2 \sin^2(q_2 + q_3)) \quad (14) \end{aligned}$$

$$C_5 = 0.5C_2 \quad (15)$$

$$C_6 = -0.5C_1 \quad (16)$$

$$C_7 = 2[-2I_9 \sin(q_3) + I_8 \cos(q_3) + I_{11} \cos(q_3)] \quad (17)$$

$$C_8 = -0.5C_4 \quad (18)$$

$$\begin{aligned} C_9 = & (1 - 2I_{10}) \sin(q_2 + q_3) \cos(q_2 + q_3) \\ & - I_{11} \cos(q_2) \cos(q_2 + q_3) \\ & - I_{12} \cos^2(q_2 + q_3) \quad (19) \end{aligned}$$

$$C_{10} = (-I_{23} + I_{19} + I_{20}) \sin(q_2 + q_3) \quad (20)$$

$$C_{11} = (-I_{20} + I_{23} + I_{19}) \sin(q_2 + q_3) \quad (21)$$

$$C_{12} = -I_{11} \cos(q_3) - I_{12} \quad (22)$$

The system gravitational parameters used in Eqs. (2)–(22) are given in Table 1. Finally, the gravity vector is

Table 1 5-DOF upper-limb exoskeleton robot parameters [1, 2]

Inertial parameters ($kg\ m^2$)	
$I_1 = 1.14 \pm 0.27$	$I_2 = 1.43 \pm 0.05$
$I_3 = 1.38 \pm 0.05$	$I_4 = 0.298 \pm 0.029$
$I_5 = -0.0213 \pm 0.0022$	$I_6 = -0.0142 \pm 0.0070$
$I_7 = -0.0001 \pm 0.0006$	$I_8 = 0.372 \pm 0.031$
$I_9 = -0.011 \pm 0.0011$	$I_{10} = 0.00125 \pm 0.0003$
$I_{11} = -0.0124 \pm 0.0003$	$I_{12} = 0.000058 \pm 0.00001$
$I_{13} = -0.69 \pm 0.02$	$I_{14} = 0.134 \pm 0.014$
$I_{15} = 0.238 \pm 0.012$	$I_{16} = 0.00379 \pm 0.0009$
$I_{17} = 0.000642 \pm 0.0003$	$I_{18} = 4.71 \pm 0.54$
$I_{19} = 1.75 \pm 0.07$	$I_{20} = 0.333 \pm 0.016$
$I_{21} = 0.000642 \pm 0.0003$	$I_{22} = 0.2 \pm 0.016$
Gravitational parameters (Nm)	
$g_1 = -37.2 \pm 0.5$	$g_2 = -8.43 \pm 0.20$
$g_3 = 1.02 \pm 0.5$	$g_4 = 0.249 \pm 0.025$
$g_5 = -0.0292 \pm 0.0056$	

given by $\mathbf{G}(\mathbf{q})^T = [0 \ G_2 \ G_3 \ 0 \ G_5]$ where

$$\begin{aligned} G_2 &= g_1 \cos(q_2) + g_3 \sin(q_2) + g_4 \cos(q_2 + q_3) \\ &\quad + (g_2 + g_5) \sin(q_2 + q_3) \end{aligned} \quad (23)$$

$$G_3 = (g_2 + g_5) \sin(q_2 + q_3) + g_4 \cos(q_2 + q_3) \quad (24)$$

$$G_5 = g_5 \sin(q_2 + q_3) \quad (25)$$

The parameters used in Eqs. (23)–(25) are given in Table 1.

Considering actuation faults, the robot dynamic model in Eq. (1) can be rewritten as follows:

$$\mathbf{M}(\mathbf{q})\ddot{\mathbf{q}} + \mathbf{C}(\mathbf{q}, \dot{\mathbf{q}})\dot{\mathbf{q}} + \mathbf{G}(\mathbf{q}) + \tau_d(\dot{\mathbf{q}}) = \tau_a \quad (26)$$

where $\tau_a \in \mathbb{R}^5$ represents the vector of actual actuation torque. Unlike in [2], in order to consider not only the partial loss of effectiveness fault, we consider that

$$\tau_a = \tau - \delta\tau + \Delta \quad (27)$$

where $\delta = \text{diag}[\delta_1, \dots, \delta_5]$ is the time-varying/constant matrix of actuation power loss rates, $\tau \in \mathbb{R}^5$ is the vector of theoretical joints input torques (provided by the control algorithm), and $\Delta^T = [\Delta_1, \dots, \Delta_5]$ represents the time-varying/constant bias in the actuation torque. Hence, Eq. (27) can represent different types of actuation faults. For $1 \leq i \leq 5$, if $\delta_i = 1$ and $\Delta_i = 0$, there is a total failure at the i -th bar-link that can manifest in free-swinging joint, or locked joint because of

jamming of bearings, transmission or because of the failure of the drive motor; if $\delta_i < 1$ and $\Delta_i = 0$, there is a partial loss of actuation at the i -th bar-link that may be caused by increased resistance in the joint movement (e.g., due to loss of lubrication) or vibrations (e.g., due to increased backlash); if $\delta_i = 1$ and $\Delta_i \neq 0$, there is a bias fault at the i -th bar-link; if $\delta_i < 1$ and $\Delta_i \neq 0$, the system may be subject to a complex fault [2, 16, 17, 45, 46].

Given a vector $\mathbf{q}_d \in \mathbb{R}^5$ of reference trajectories for the five links, the objective is to design a controller that will provide $\tau \in \mathbb{R}^5$ to force the robot position vector $\mathbf{q} \in \mathbb{R}^5$ to track \mathbf{q}_d with accuracy despite the torque disturbance $\tau_d \in \mathbb{R}^5$, unknown or uncertain system dynamics or parameters ($\mathbf{M}(\mathbf{q})$, $\mathbf{C}(\mathbf{q}, \dot{\mathbf{q}})$, and $\mathbf{G}(\mathbf{q})$), unavailable velocity measurements $\dot{\mathbf{q}}$, actuation faults of different types.

2.2 Controller design: ideal case with available states and system dynamics

Here we first assume that full system state measurement information (\mathbf{q} , $\dot{\mathbf{q}}$) and system nonlinear dynamics (or parameters $\mathbf{M}(\mathbf{q})$, $\mathbf{C}(\mathbf{q}, \dot{\mathbf{q}})$, and $\mathbf{G}(\mathbf{q})$) are known. This will set the path to the main results of this paper.

Considering the aforementioned control objective, let us denote the position tracking error vector by $\mathbf{e}^T = [e_1, \dots, e_5]$ where $e_i = q_{d,i} - q_i$ for $1 \leq i \leq 5$.

Let us denote the sliding function vector as $\mathbf{s}^T = [s_1, \dots, s_5]$ obtained from

$$\mathbf{s} = \dot{\mathbf{e}} + \boldsymbol{\Gamma}\mathbf{e} \quad (28)$$

where $\boldsymbol{\Gamma} = \boldsymbol{\Gamma}^T \in \mathbb{R}^{5 \times 5}$ is a positive-definite constant diagonal matrix. The first time derivative of \mathbf{s} multiplied by the generalized inertia matrix corresponds to

$$\mathbf{M}(\mathbf{q})\dot{\mathbf{s}} = \mathbf{M}(\mathbf{q})(\ddot{\mathbf{q}}_d + \boldsymbol{\Gamma}\dot{\mathbf{e}}) - \mathbf{M}(\mathbf{q})\ddot{\mathbf{q}} \quad (29)$$

Using the expression of $\ddot{\mathbf{q}}$ obtained from Eq. (26), we obtain

$$\begin{aligned} \mathbf{M}(\mathbf{q})\dot{\mathbf{s}} &= \mathbf{M}(\mathbf{q})(\ddot{\mathbf{q}}_d + \boldsymbol{\Gamma}\dot{\mathbf{e}}) + \mathbf{C}(\mathbf{q}, \dot{\mathbf{q}})\dot{\mathbf{q}} + \mathbf{G}(\mathbf{q}) \\ &\quad + \tau_d(\dot{\mathbf{q}}) - \tau_a \end{aligned} \quad (30)$$

Using Eq. (27) in Eq. (30), we obtain

$$\begin{aligned} \mathbf{M}(\mathbf{q})\dot{\mathbf{s}} &= \mathbf{M}(\mathbf{q})(\ddot{\mathbf{q}}_d + \boldsymbol{\Gamma}\dot{\mathbf{e}}) + \mathbf{C}(\mathbf{q}, \dot{\mathbf{q}})\dot{\mathbf{q}} \\ &\quad + \mathbf{G}(\mathbf{q}) + \psi(\dot{\mathbf{q}}, \tau) - \tau \end{aligned} \quad (31)$$

where $\psi(\dot{\mathbf{q}}, \tau) = \tau_d(\dot{\mathbf{q}}) + \delta \cdot \tau - \Delta$ is the lumped disturbance, resulting from the disturbance torque and the actuation fault.

Here we propose the use of a sliding mode reaching law given as follows:

$$\mathbf{M}(\mathbf{q})\dot{\mathbf{s}} = -\eta\mathbf{T}(\mathbf{s}) - \mathbf{KE}(\mathbf{s}) \quad (32)$$

where $\eta = \text{diag}[\eta_1, \dots, \eta_5]$ and $\mathbf{K} = \text{diag}[K_1, \dots, K_5]$ are positive-definite design matrices, $\mathbf{T}(\mathbf{s})^T = [T_1(s_1), \dots, T_5(s_5)]$ with

$$T_i(s_i) = \frac{\exp(4s_i) - 1}{\exp(4s_i) + 1} \quad (33)$$

and $\mathbf{E}(\mathbf{s})^T = [E_1(s_1), \dots, E_5(s_5)]$ with

$$E_i(s_i) = \frac{s_i}{\exp(s_i) + 1} \quad (34)$$

Using the reaching law given by Eq. (32), we obtain chattering phenomenon cancelation without involving some chattering avoidance methods that have been reported to alter the controllers' robustness feature and that may involve some additional design parameters to the control system that may need to be tuned [40, 48]. Some of these methods consist in, for instance, replacing the sign function of the traditional SMC with a boundary layer function [20, 49] or saturation function [40, 43], using a continuous hyperbolic tangent function [50], using fuzzy logic to adjust the slope of switching surface [51], using a disturbance observer [52], using a radial basis function neural network [53], and/or using power rate reaching strategy [54].

Using Eq. (31) (where $\psi(\dot{\mathbf{q}}, \tau) = 0$) and Eq. (32), we derive the joints theoretical input torque vector as follows

$$\tau = \mathbf{f}(\mathbf{q}, \dot{\mathbf{q}}) + \eta\mathbf{T}(\mathbf{s}) + \mathbf{KE}(\mathbf{s}) \quad (35)$$

where the nonlinear function vector $\mathbf{f}(\mathbf{q}, \dot{\mathbf{q}}) \in \mathbb{R}^5$ corresponds to

$$\mathbf{f}(\mathbf{q}, \dot{\mathbf{q}}) = \mathbf{M}(\mathbf{q})(\ddot{\mathbf{q}}_d + \Gamma\dot{\mathbf{e}}) + \mathbf{C}(\mathbf{q}, \dot{\mathbf{q}})\dot{\mathbf{q}} + \mathbf{G}(\mathbf{q}) \quad (36)$$

In order to check under which condition the control law given by Eq. (35) can guarantee the closed-loop system stability, let us consider the following Lyapunov function

$$V = \frac{1}{2}\mathbf{s}^T \mathbf{M}(\mathbf{q})\mathbf{s} \quad (37)$$

The first time derivative of this function is

$$\begin{aligned} \dot{V} &= \mathbf{s}^T \mathbf{M}(\mathbf{q})\dot{\mathbf{s}} + \frac{1}{2}\mathbf{s}^T \dot{\mathbf{M}}(\mathbf{q})\mathbf{s} \\ &= \mathbf{s}^T \mathbf{M}(\mathbf{q})\dot{\mathbf{s}} + \frac{1}{2}\mathbf{s}^T (\dot{\mathbf{M}}(\mathbf{q}) - 2\mathbf{C}(\mathbf{q}, \dot{\mathbf{q}}))\mathbf{s} \\ &= \mathbf{s}^T \mathbf{M}(\mathbf{q})\dot{\mathbf{s}} \end{aligned} \quad (38)$$

Let us apply Eq. (35) in Eq. (31) (where $\psi(\dot{\mathbf{q}}, \tau) \neq 0$) to obtain

$$\mathbf{M}(\mathbf{q})\dot{\mathbf{s}} = \psi(\dot{\mathbf{q}}, \tau) - \eta\mathbf{T}(\mathbf{s}) - \mathbf{KE}(\mathbf{s}) \quad (39)$$

Applying Eq. (39) in Eq. (38), we obtain

$$\dot{V} = \mathbf{s}^T [\psi(\dot{\mathbf{q}}, \tau) - \eta\mathbf{T}(\mathbf{s}) - \mathbf{KE}(\mathbf{s})] \quad (40)$$

Considering the worst-case scenario caused by the disturbance $\psi(\dot{\mathbf{q}}, \tau)$, the sliding variable may go away from the origin such that $T_i(s_i) = \frac{\exp(4s_i)-1}{\exp(4s_i)+1} \approx 1$. Therefore, Eq. (40) becomes

$$\begin{aligned} \dot{V} &\approx \mathbf{s}^T \psi(\dot{\mathbf{q}}, \tau) - \mathbf{s}^T \eta \mathbf{I}_5 - \sum_{i=1}^5 K_i \frac{s_i^2}{\exp(s_i) + 1} \\ &\leq \|\mathbf{s}\| (\|\psi(\dot{\mathbf{q}}, \tau)\|_{\max} - \|\eta\|) - \sum_{i=1}^5 K_i \frac{s_i^2}{\exp(s_i) + 1} \end{aligned} \quad (41)$$

If we select the five diagonal elements of the positive-definite matrix η such that, $\eta_i > |\psi_i(\dot{q}_i, \tau_i)|_{\max}$ for $1 \leq i \leq 5$, with $K_i \in \mathbb{R}^+$, we obtain $\dot{V} \leq 0$. Therefore, under this condition, the closed-loop system asymptotic stability is guaranteed. Thus, according to Barbalat's lemma, $\mathbf{s} \rightarrow 0$, $\mathbf{e} \rightarrow 0$ as $t \rightarrow \infty$, despite torque disturbances and actuation faults.

Remark 1 The implementation of the designed control law Eq. (35) requires the availability of full-state measurements $(\mathbf{q}, \dot{\mathbf{q}})$, the exact knowledge of the system dynamics $\mathbf{f}(\mathbf{q}, \dot{\mathbf{q}})$ given by Eq. (36), and the knowledge of the upper bound of the lumped disturbance $\psi(\dot{\mathbf{q}}, \tau)$. This requirement is unlikely to be fulfilled in practical applications because of the uncertain nature of the upper-limb exoskeleton robot, the unavailability

of the full-state measurement, and the unknown disturbance upper bound. Therefore, the control law Eq. (35) should be improved by making its implementation independent of full-state measurement availability, systems dynamics, and disturbances bounds. This improvement is the main subject of the next section.

3 Main results

3.1 High-gain state observer design

Having only information on robot links position vector \mathbf{q} , let us use a high-gain state observer that will provide an accurate estimation $\dot{\hat{\mathbf{q}}}$ of the unavailable velocity vector $\dot{\mathbf{q}}$. Let us first consider the state-space representation of the robot dynamic model by rewriting Eq. (26) as follows:

$$\begin{cases} \dot{\mathbf{x}} = \mathbf{A}\mathbf{x} + \mathbf{F}(\mathbf{x}, \tau) \\ \mathbf{y} = \mathbf{H}\mathbf{x} \end{cases} \quad (42)$$

where $\mathbf{x}^T = [\mathbf{x}_1^T, \dots, \mathbf{x}_5^T]$ is the state vector with $\mathbf{x}_i^T = [q_i \dot{q}_i]$; $\mathbf{y} \in \mathbb{R}^5$ is the system output vector; $\mathbf{F}(\mathbf{x}, \tau) = -\mathbf{B} \cdot \mathbf{M}^{-1}(\mathbf{q}) [\mathbf{C}(\mathbf{q}, \dot{\mathbf{q}})\dot{\mathbf{q}} + \mathbf{G}(\mathbf{q}) + \tau_d(\dot{\mathbf{q}}) - \tau_a]$; for $1 \leq i \leq 5$, $\mathbf{A} = \text{diag}[\mathbf{A}_1, \dots, \mathbf{A}_5]$ with $\mathbf{A}_i = \begin{bmatrix} 0 & 1 \\ 0 & 0 \end{bmatrix}$, $\mathbf{B} = \text{diag}[\mathbf{B}_1, \dots, \mathbf{B}_5]$ with $\mathbf{B}_i = \begin{bmatrix} 0 \\ 1 \end{bmatrix}$, and $\mathbf{H} = \text{diag}[\mathbf{H}_1, \dots, \mathbf{H}_5]$ with $\mathbf{H}_i = [1 \ 0]$ such that \mathbf{H} is a full rank matrix in accordance with the observability criteria.

Assumption 1 [18, 19, 58–60] With the state vector $\mathbf{x} \in \mathbb{R}^{10}$ bounded over the compact set $\Omega \subset \mathbb{R}^{10}$, and the control torque $\tau \in \mathbb{R}^5$ restricted to the class of admissible control torques $U \in \mathbb{R}^5$, the nonlinear vector field $\mathbf{F}(\mathbf{x}, \tau)$ is bounded with respect to its arguments on Ω , i.e., there exist a positive scalar valued function $\rho(\mathbf{x}, \tau)$ such that $\|\mathbf{F}(\mathbf{x}, \tau)\| \leq \|\mathbf{P}\|^{-1} \rho(\mathbf{x}, \tau)$ $\forall \mathbf{x} \in \mathbb{R}^{10}$ and $\forall \tau \in \mathbb{R}^5$, with $\mathbf{P} = \mathbf{P}^T > 0$.

Knowing that the system dynamics are unavailable and that only position information \mathbf{q} is available, the objective is to design an observer that does not involve the system dynamics in its implementation, for which the input is the system output vector \mathbf{y} , and for which the state $\hat{\mathbf{x}}$ will converge asymptotically to \mathbf{x} , i.e., $\lim_{t \rightarrow \infty} (\hat{\mathbf{x}} - \mathbf{x}) = 0$. For that we use a high-gain observer modeled by

$$\begin{cases} \dot{\hat{\mathbf{x}}} = \mathbf{A}\hat{\mathbf{x}} + \mathbf{L}(\mathbf{y} - \hat{\mathbf{y}}) \\ \hat{\mathbf{y}} = \mathbf{H}\hat{\mathbf{x}} \end{cases} \quad (43)$$

where $\mathbf{L} = \text{block-diag}[\mathbf{L}_1, \dots, \mathbf{L}_5]$ is the high-gain observer matrix with $\mathbf{L}_i^T = \begin{bmatrix} k_{i,1} & k_{i,2} \\ \epsilon(t) & \epsilon(t)^2 \end{bmatrix}$. The parameters $k_{i,1}$ and $k_{i,2}$ are selected such that the polynomial $p^2 + k_{i,2}p + k_{i,1} = 0$ is Hurwitz. The time-varying parameter $\epsilon(t) \in \mathbb{R}^+$ is expressed as follows [25]:

$$\epsilon(t) = \frac{\exp(50t) + 1}{100 [\exp(50t) - 1]} \quad (44)$$

Let us denote $\tilde{\mathbf{x}} = \mathbf{x} - \hat{\mathbf{x}}$ the state estimation error vector. Using Eqs. (42) and (43), the dynamics of this error is given as follows:

$$\begin{aligned} \dot{\tilde{\mathbf{x}}} &= \dot{\mathbf{x}} - \dot{\hat{\mathbf{x}}} \\ &= (\mathbf{A} - \mathbf{LH})\tilde{\mathbf{x}} + \mathbf{F}(\mathbf{x}, \tau) \\ &= \mathbf{A}_0\tilde{\mathbf{x}} + \mathbf{F}(\mathbf{x}, \tau) \end{aligned} \quad (45)$$

where $\mathbf{A}_0 = (\mathbf{A} - \mathbf{LH})$ has all its eigenvalues with negative real parts.

In order to check the convergence property of the state observer, let use the following Lyapunov function:

$$V = \frac{1}{2}\tilde{\mathbf{x}}^T \mathbf{P}\tilde{\mathbf{x}} \quad (46)$$

where $\mathbf{P} = \mathbf{P}^T > 0 \in \mathbb{R}^{10 \times 10}$, mentioned in Assumption 1, is a solution of the following Riccati algebraic equation:

$$\mathbf{A}_0^T \mathbf{P} + \mathbf{P} \mathbf{A}_0 = -\mathbf{Q} \quad (47)$$

for a given $\mathbf{Q} = \mathbf{Q}^T > 0 \in \mathbb{R}^{10 \times 10}$. The first time derivative of the Lyapunov function is

$$\begin{aligned} \dot{V} &= \frac{1}{2}\dot{\tilde{\mathbf{x}}}^T \mathbf{P}\tilde{\mathbf{x}} + \frac{1}{2}\tilde{\mathbf{x}}^T \mathbf{P}\dot{\tilde{\mathbf{x}}} \\ &= \frac{1}{2}\tilde{\mathbf{x}}^T (\mathbf{A}_0^T \mathbf{P} + \mathbf{P} \mathbf{A}_0) \tilde{\mathbf{x}} + \tilde{\mathbf{x}}^T \mathbf{P} \mathbf{F}(\mathbf{x}, \tau) \end{aligned} \quad (48)$$

Using Eq. (47), under Assumption 1, Eq. (48) becomes

$$\begin{aligned} \dot{V} &= -\frac{1}{2}\tilde{\mathbf{x}}^T \mathbf{Q}\tilde{\mathbf{x}} + \tilde{\mathbf{x}}^T \mathbf{P} \mathbf{F}(\mathbf{x}, \tau) \\ &\leq -\frac{1}{2}\tilde{\mathbf{x}}^T \mathbf{Q}\tilde{\mathbf{x}} + \|\tilde{\mathbf{x}}\| \|\mathbf{P}\| \|\mathbf{F}(\mathbf{x}, \tau)\| \end{aligned}$$

$$\begin{aligned} &\leq -\frac{1}{2}\tilde{\mathbf{x}}^T \mathbf{Q}\tilde{\mathbf{x}} + \|\tilde{\mathbf{x}}\|\rho(\mathbf{x}, \tau) \\ &\leq -\frac{1}{2}\lambda_{\min}(\mathbf{Q})\|\tilde{\mathbf{x}}\|^2 + \|\tilde{\mathbf{x}}\|\rho(\mathbf{x}, \tau) \end{aligned} \quad (49)$$

where $\lambda_{\min}(\mathbf{Q})$ is the smallest eigenvalue of \mathbf{Q} . Therefore, we have $\dot{V} \leq 0$ whenever $\|\tilde{\mathbf{x}}\|$ is outside the region bounded by $\|\tilde{\mathbf{x}}\| \leq 2\rho(\mathbf{x}, \tau)/\lambda_{\min}(Q)$. Hence, according to the Barbalat's lemma, $\forall t \geq 0, \lim_{t \rightarrow \infty} (\mathbf{x} - \hat{\mathbf{x}}) = 0$ such that $\hat{\mathbf{x}}$ is guaranteed to be bounded in the compact set Ω . This convergence property is illustrated by the simulation results presented in Sect. 4.

3.2 Fuzzy neural network and observer-based nonlinear controller design

As stated by Remark 1 of Sect. 2, the control law given by Eq. (35) is not good for practical applications as the robot dynamics $\mathbf{f}(\mathbf{q}, \dot{\mathbf{q}})$, the full-state vector \mathbf{x} , and the disturbance torque and actuation fault upper bounds ($\|\psi(\dot{\mathbf{q}}, \tau)\|_{\max}$) are not available. Therefore, we exploit the state observer given by Eq. (43) to obtain an accurate estimation $\hat{\mathbf{x}}$ of the state vector \mathbf{x} .

In order to approximate the unknown dynamics with the approximate state vector $(\mathbf{f}(\hat{\mathbf{q}}, \dot{\hat{\mathbf{q}}}))$, considering that the approximate state vector $\hat{\mathbf{x}}$ remains bounded in the compact set $\Omega \in \mathbb{R}^{10} \forall t$, we exploit the universal approximation theorem of FNN (in this paper, unlike in [21, 55], the FNN is used for approximating only one nonlinear vector function: less computational burden). FNN are known for their ability of exploiting the structural advantage of fuzzy logic systems and the learning capability of neural networks [61]. It has been proved several times that FNN are able to approximate any continuous nonlinear function defined on a compact set Ω to arbitrary accuracy (see, for instance, in [20, 21, 24, 34, 41, 56, 57, 62]).

With a FNN using a center-of-gravity defuzzification method, an approximation of the nonlinear vector function is obtained as $\hat{\mathbf{f}}(\hat{\mathbf{q}}, \dot{\hat{\mathbf{q}}})^T = [f_1, \dots, f_5]$ where, for $i = 1, \dots, 5$, we have:

$$\begin{aligned} \hat{f}_i(\mathbf{x}_{ei}|\hat{\theta}_i) &= \frac{\sum_{j=1}^m \hat{\theta}_{i,j}(t) \left(\prod_{l=1}^k \mu_{A_l^j}(x_{ei,l}) \right)}{\sum_{j=1}^m \left(\prod_{l=1}^k \mu_{A_l^j}(x_{ei,l}) \right)} \\ &= \hat{\theta}_i^T(t) \varphi(\mathbf{x}_{ei}) \end{aligned} \quad (50)$$

with m being the number of fuzzy rules, k being the length of the FNN input vector \mathbf{x}_{ei} for the i th link. In this paper, $\mathbf{x}_{ei} = [q_{d,i} - \hat{q}_i, \dot{q}_{d,i} - \dot{\hat{q}}_i]$; the FNN weighting vector for the i th link is $\hat{\theta}_i^T(t) = [\hat{\theta}_{i1}(t), \dots, \hat{\theta}_{im}(t)]$; $\varphi(\mathbf{x}_{ei}) \in \mathbb{R}^m$ is the vector of fuzzy basis functions for the i th link, for which the components $\varphi_j(\mathbf{x}_{ei})$, for $1 \leq j \leq m$, are obtained from:

$$\varphi_i(\mathbf{x}_{ei}) = \frac{\prod_{l=1}^k \mu_{A_l^j}(x_{ei,l})}{\sum_{j=1}^m \left(\prod_{l=1}^k \mu_{A_l^j}(x_{ei,l}) \right)} \quad (51)$$

where A_l^j are the fuzzy sets that correspond to the membership functions $\mu_{A_l^j}$, for $1 \leq l \leq k$ and $1 \leq j \leq m$, calculated for each input $x_{ei,l}$ using the Gaussian function given as follows:

$$\mu_{A_l^j}(x_{ei,l}) = \exp \left[-\frac{(x_{ei,l} - a_{i,l}^j)^2}{2\mu^2} \right] \quad (52)$$

where $a_{i,l}^j$ is the width of the Gaussian function and $\mu > 0$ is the center of the receptive field. These parameters, known as membership function parameter set, and the number of fuzzy rules (m) are very relevant for the accuracy of the FNN output. The approximate vector function at the output of the FNN can therefore be written as follows

$$\hat{\mathbf{f}}(\mathbf{x}_e|\hat{\theta}) = \hat{\theta}^T \varphi(\mathbf{x}_e) \quad (53)$$

where $\varphi^T = [\varphi^T(\mathbf{x}_{e1}), \dots, \varphi^T(\mathbf{x}_{e5})] \in \mathbb{R}^{5 \cdot m}$, and $\hat{\theta} = \text{block-diag}[\hat{\theta}_1, \dots, \hat{\theta}_5] \in \mathbb{R}^{5 \cdot m \times 5}$ is the matrix of the five links weighting vectors, for which the update law is designed as follows:

$$\dot{\hat{\theta}} = \gamma^{-1} \varphi(\mathbf{x}_e) \hat{\mathbf{s}}^T \quad (54)$$

with $\hat{\mathbf{s}} \in \mathbb{R}^5$ being the sliding function vector obtained with the estimated states as follows:

$$\dot{\hat{\mathbf{s}}} = \dot{\hat{e}} + \Gamma \hat{e} \quad (55)$$

where $\hat{\mathbf{e}}^T = [\hat{e}_1, \dots, \hat{e}_5]$, with $\hat{e}_i = q_{d,i} - \hat{q}_i$, is the approximate tracking error vector; $\gamma = \text{diag}[\gamma_1, \dots, \gamma_5]$, with $\gamma_i > 0 \in \mathbb{R}$ ($1 \leq i \leq 5$) being the learning rate for the dynamics of the i th link.

The benefit of using the update law expressed by Eq. (54), which is a function of the approximate closed-loop system tracking error dynamics, is that the parameter $\hat{\theta}(t)$ does not have a direct effect on the closed-loop system stability (see the proof of Theorem 1). This dynamics of \hat{e} is defined by the sliding function given by Eq. (55) where the parameter $\Gamma = \Gamma^T > 0 \in \mathbb{R}^{5 \times 5}$ is selected such that $\lim_{t \rightarrow \infty} \hat{e} = 0$.

The difference between the FNN output given by Eq. (53) and the exact nonlinear function given by Eq. (36) corresponds to:

$$\hat{\mathbf{f}}(\mathbf{x}_e|\hat{\theta}) - \mathbf{f}(\mathbf{q}, \dot{\mathbf{q}}) = \tilde{\theta}^T \varphi(\mathbf{x}_e) - \varepsilon(\mathbf{x}_e) \quad (56)$$

where $\tilde{\theta}(t)$ is the error on approximated weight matrix $\hat{\theta}(t)$, $\varepsilon^T(\mathbf{x}_e) = [\varepsilon_1(\mathbf{x}_{e1}), \dots, \varepsilon_5(\mathbf{x}_{e5})]$ is the FNN approximation error vector.

Assumption 2 The approximation errors $\varepsilon_i(\mathbf{x}_{ei})$ are bounded by some unknown constants $\varepsilon_{i \max} > 0$ over the compact set $\Omega \in R^{10}$, i.e., $\max_{\mathbf{x}_{ei} \in \Omega} |\varepsilon_i(\mathbf{x}_{ei})| \leq \varepsilon_{i \max}$.

In order to improve the FNN performances (i.e., to compensate the approximation error effects) for a fixed low number of fuzzy rules m and a fixed FNN parameter set, we add to the designed control law a dynamic parameter vector $\hat{e}(t) \in \mathbb{R}^5$ tuned online to compensate the FNN approximation errors without causing an important computational load, while ensuring robustness of the control system (and without any prior error upper bound knowledge). The update rule for this parameter vector is

$$\dot{\hat{e}}(t) = \zeta_\varepsilon^{-1} \hat{s} \quad (57)$$

where $\zeta_\varepsilon = \text{diag}[\zeta_{\varepsilon,1}, \dots, \zeta_{\varepsilon,5}]$, with $\zeta_{\varepsilon,i} \in \mathbb{R}^+$ (for $1 \leq i \leq 5$), is the matrix of the parameter $\hat{e}(t)$ learning rate.

In order to compensate the effects of the lumped disturbance $\psi(\dot{\mathbf{q}}, \tau)$ without any prior knowledge of its upper bound, unlike as suggested in Sect. 2, let us add to the control law the dynamic matrix $\hat{\eta}_1(t) = \text{diag}[\hat{\eta}_{1,1}, \dots, \hat{\eta}_{1,5}]$ for which the update rule is

$$\dot{\hat{\eta}}_1 = \zeta_\eta^{-1} \hat{s}^* \quad (58)$$

where $\hat{s}^* = \text{diag}[\hat{s}_1, \dots, \hat{s}_5]$, $\zeta_\eta = \text{diag}[\zeta_{\eta,1}, \dots, \zeta_{\eta,5}]$, with $\zeta_{\eta,i} \in \mathbb{R}^+$ (for $1 \leq i \leq 5$), is the matrix of the parameter $\hat{\eta}_1(t)$ learning rate.

Theorem 1 By generating the robot actuation input torque using the following control law

$$\tau = \hat{\mathbf{f}}(\mathbf{x}_e|\hat{\theta}) + \hat{\eta}(t) T(\hat{\mathbf{s}}) + \mathbf{KE}(\hat{\mathbf{s}}) \quad (59)$$

that uses the estimated vector $\hat{\mathbf{x}} \in \mathbb{R}^{10}$ of the high-gain state observer given by Eq. (43) (with proved convergence) and the FNN output given by Eq. (53) for which the weights are adjusted using Eq. (54), the closed-loop system's stability, and therefore, robustness is guaranteed regardless the changes in the robotic system's parameters, the torque disturbances, the FNN approximation error, and different types of actuation faults; this is ensured if

$$\hat{\eta}(t) = \hat{\eta}_1(t) + \eta_2(t) \quad (60)$$

with $\hat{\eta}_1(t) \in \mathbb{R}^{5 \times 5}$ obtained using the update rule by Eq. (58), and $\eta_2(t) = \text{diag}[\varrho|\hat{\varepsilon}_1|, \dots, \varrho|\hat{\varepsilon}_5|]$, with $\varrho > 1 \in \mathbb{R}$, where the parameters $\hat{\varepsilon}_i$ are obtained using the update rule in Eq. (57); $\mathbf{K} = \text{diag}[K_1, \dots, K_5] > 0$, $\mathbf{T}(\hat{\mathbf{s}}) \in \mathbb{R}^5$ and $\mathbf{E}(\hat{\mathbf{s}}) \in \mathbb{R}^5$ are obtained using Eqs. (33) and (34), respectively.

Proof in order to prove Theorem 1, let us consider the following candidate Lyapunov function (*in the following development, for simplicity in notations, we will omit the independent variable t , and the dependent variables \mathbf{q} and $\dot{\mathbf{q}}$*):

$$V = V_1 + V_2 \quad (61)$$

where

$$V_1 = \frac{1}{2} \mathbf{s}^T \mathbf{M} \mathbf{s} + \frac{1}{2} \text{tr} \left[\tilde{\theta}^T \gamma \tilde{\theta} \right] \quad (62)$$

with the error vector on the approximate weight $\hat{\theta}$ given as

$$\tilde{\theta} = \hat{\theta} - \theta^* \quad (63)$$

where $\theta^* \in \mathbb{R}^{5 \cdot m \times 5}$ is the optimal weight vector, which is used here only for stability analysis purpose, and

$$V_2 = \frac{1}{2} \text{tr} \left[\tilde{\eta}_1^T \zeta_\eta \tilde{\eta}_1 \right] + \frac{1}{2} \tilde{\varepsilon}^T \zeta_\varepsilon \tilde{\varepsilon} \quad (64)$$

with the error on the approximate matrix $\hat{\eta}_1$ given by

$$\tilde{\eta}_1 = \hat{\eta}_1 - \eta_1 \quad (65)$$

with η_1 being a large value considered here only for analytical purpose, and

$$\tilde{\varepsilon} = \hat{\varepsilon} - \varepsilon(\mathbf{x}_e) \quad (66)$$

is the error matrix on the approximate $\hat{\varepsilon}$.

Let us find the first-order derivative of V_1 and apply the identity given by Eq. (63) as follows:

$$\begin{aligned} \dot{V}_1 &= \mathbf{s}^T \mathbf{M} \dot{\mathbf{s}} + \frac{1}{2} \mathbf{s}^T \dot{\mathbf{M}} \mathbf{s} + \text{tr} \left[\tilde{\theta}^T \gamma \dot{\tilde{\theta}} \right] \\ &= \mathbf{s}^T \mathbf{M} \dot{\mathbf{s}} + \frac{1}{2} \mathbf{s}^T (\dot{\mathbf{M}} - 2\mathbf{C}) \mathbf{s} + \text{tr} \left[\tilde{\theta}^T \gamma \dot{\tilde{\theta}} \right] \\ &= \mathbf{s}^T \mathbf{M} \dot{\mathbf{s}} + \text{tr} \left[\tilde{\theta}^T \gamma \dot{\tilde{\theta}} \right] \end{aligned} \quad (67)$$

Let us apply the control law given by Eq. (59) in Eq. (31) [where the identities Eqs. (36) and (56) are used] to obtain

$$\mathbf{M} \dot{\mathbf{s}} = - \left[\tilde{\theta}^T \varphi(\mathbf{x}_e) - \varepsilon(\mathbf{x}_e) \right] + \psi - \hat{\eta} \mathbf{T}(\hat{\mathbf{s}}) - \mathbf{KE}(\hat{\mathbf{s}}) \quad (68)$$

Applying Eq. (68) in Eq. (67), we obtain

$$\begin{aligned} \dot{V}_1 &= \mathbf{s}^T \left\{ - \left[\tilde{\theta}^T \varphi(\mathbf{x}_e) - \varepsilon(\mathbf{x}_e) \right] + \psi - \hat{\eta} \mathbf{T}(\hat{\mathbf{s}}) \right. \\ &\quad \left. - \mathbf{KE}(\hat{\mathbf{s}}) \right\} + \text{tr} \left[\tilde{\theta}^T \gamma \dot{\tilde{\theta}} \right] \\ &= \text{tr} \left[\tilde{\theta}^T \left(\gamma \dot{\tilde{\theta}} - \varphi(\mathbf{x}_e) \mathbf{s}^T \right) \right] + \mathbf{s}^T \varepsilon(\mathbf{x}_e) + \mathbf{s}^T \psi \\ &\quad - \mathbf{s}^T \hat{\eta} \mathbf{T}(\hat{\mathbf{s}}) - \mathbf{s}^T \mathbf{KE}(\hat{\mathbf{s}}) \end{aligned} \quad (69)$$

Applying the update law given by Eq. (54) in Eq. (69) yields

$$\begin{aligned} \dot{V}_1 &= \text{tr} \left[\tilde{\theta}^T \varphi(\mathbf{x}_e) \left(\hat{\mathbf{s}}^T - \mathbf{s}^T \right) \right] + \mathbf{s}^T \varepsilon(\mathbf{x}_e) + \mathbf{s}^T \psi \\ &\quad - \mathbf{s}^T \hat{\eta} \mathbf{T}(\hat{\mathbf{s}}) - \mathbf{s}^T \mathbf{KE}(\hat{\mathbf{s}}) \end{aligned} \quad (70)$$

Considering the convergence property of the employed high-gain state observer, i.e., the fact that $\hat{\mathbf{s}} \rightarrow \mathbf{s}$, we have

$$\dot{V}_1 = \mathbf{s}^T \varepsilon(\mathbf{x}_e) + \mathbf{s}^T \psi - \mathbf{s}^T \hat{\eta} \mathbf{T}(\hat{\mathbf{s}}) - \mathbf{s}^T \mathbf{KE}(\hat{\mathbf{s}}) \quad (71)$$

The first time derivative of Eq. (64) corresponds to

$$\dot{V}_2 = \text{tr} \left[\tilde{\eta}_1^T \zeta_\eta \dot{\tilde{\eta}}_1 \right] + \tilde{\varepsilon}^T \zeta_\varepsilon \dot{\tilde{\varepsilon}} \quad (72)$$

Using Eqs. (65), (66), (71), and (72), the first time derivative of the Lyapunov function given by Eq. (61) can be written as follows:

$$\begin{aligned} \dot{V} &= \mathbf{s}^T (\hat{\varepsilon} - \tilde{\varepsilon}) + \mathbf{s}^T \psi - \mathbf{s}^T \hat{\eta} \mathbf{T}(\hat{\mathbf{s}}) - \mathbf{s}^T \mathbf{KE}(\hat{\mathbf{s}}) \\ &\quad + \text{tr} \left[\tilde{\eta}_1^T \zeta_\eta \dot{\tilde{\eta}}_1 \right] + \tilde{\varepsilon}^T \zeta_\varepsilon \dot{\tilde{\varepsilon}} \\ &= \tilde{\varepsilon}^T \left(\zeta_\varepsilon \dot{\hat{\varepsilon}} - \mathbf{s} \right) + \mathbf{s}^T \psi - \mathbf{s}^T \hat{\eta} \mathbf{T}(\hat{\mathbf{s}}) - \mathbf{s}^T \mathbf{KE}(\hat{\mathbf{s}}) \\ &\quad + \text{tr} \left[\tilde{\eta}_1^T \zeta_\eta \dot{\tilde{\eta}}_1 \right] + \mathbf{s}^T \hat{\varepsilon} \end{aligned} \quad (73)$$

Let us apply the update rule given by Eq. (57) in Eq. (73) to obtain

$$\begin{aligned} \dot{V} &= \tilde{\varepsilon}^T (\hat{\mathbf{s}} - \mathbf{s}) + \mathbf{s}^T \psi - \mathbf{s}^T \hat{\eta} \mathbf{T}(\hat{\mathbf{s}}) - \mathbf{s}^T \mathbf{KE}(\hat{\mathbf{s}}) \\ &\quad + \text{tr} \left[\tilde{\eta}_1^T \zeta_\eta \dot{\tilde{\eta}}_1 \right] + \mathbf{s}^T \hat{\varepsilon} \end{aligned} \quad (74)$$

Considering the convergence property of the state observer, i.e., $\hat{\mathbf{s}} \rightarrow \mathbf{s}$, we have

$$\dot{V} = \mathbf{s}^T \psi - \mathbf{s}^T \hat{\eta} \mathbf{T}(\hat{\mathbf{s}}) - \mathbf{s}^T \mathbf{KE}(\hat{\mathbf{s}}) + \text{tr} \left[\tilde{\eta}_1^T \zeta_\eta \dot{\tilde{\eta}}_1 \right] + \mathbf{s}^T \hat{\varepsilon} \quad (75)$$

Considering the worst-case scenario caused by the disturbance $\psi(\hat{\mathbf{q}}, \tau)$, the sliding variable $\hat{\mathbf{s}}$ may go away from the origin such that $T_i(\hat{s}_i) = \frac{\exp(4\hat{s}_i) - 1}{\exp(4\hat{s}_i) + 1} \approx 1$. Therefore, Eq. (75) can be written as follows:

$$\begin{aligned} \dot{V} &\approx \mathbf{s}^T \psi - \mathbf{s}^T \hat{\eta} \mathbf{I}_5 - \mathbf{s}^T \mathbf{KE}(\hat{\mathbf{s}}) + \text{tr} \left[\tilde{\eta}_1^T \zeta_\eta \dot{\tilde{\eta}}_1 \right] + \mathbf{s}^T \hat{\varepsilon} \\ &= \mathbf{s}^T \psi - \mathbf{s}^T (\hat{\eta}_1 + \eta_2) \mathbf{I}_5 - \sum_{i=1}^5 K_i \frac{\hat{s}_i s_i}{\exp(\hat{s}_i) + 1} \\ &\quad + \text{tr} \left[\tilde{\eta}_1^T \zeta_\eta \dot{\tilde{\eta}}_1 \right] + \mathbf{s}^T \hat{\varepsilon} - \mathbf{s}^T \eta_1 \mathbf{I}_5 + \mathbf{s}^T \eta_1 \mathbf{I}_5 \end{aligned} \quad (76)$$

Applying the identities Eqs. (60) and (65), and considering the convergence of the observer, i.e., $s = \hat{s}$, Eq. (76) becomes as follows

$$\begin{aligned} \dot{V} &= \mathbf{s}^T (-\hat{\eta}_1 + \eta_1) \mathbf{I}_5 - \sum_{i=1}^5 K_i \frac{s_i^2}{\exp(s_i) + 1} \\ &\quad + \mathbf{s}^T \psi + \text{tr} \left[\tilde{\eta}_1^T \zeta_\eta \dot{\tilde{\eta}}_1 \right] + \mathbf{s}^T \hat{\varepsilon} - \mathbf{s}^T \eta_1 \mathbf{I}_5 - \mathbf{s}^T \eta_2 \mathbf{I}_5 \\ &= -\mathbf{s}^T \tilde{\eta}_1 \mathbf{I}_5 - \sum_{i=1}^5 K_i \frac{s_i^2}{\exp(s_i) + 1} + \mathbf{s}^T \hat{\varepsilon} \\ &\quad + \mathbf{s}^T \psi + \text{tr} \left[\tilde{\eta}_1^T \zeta_\eta \dot{\tilde{\eta}}_1 \right] - \mathbf{s}^T \eta_1 \mathbf{I}_5 - \mathbf{s}^T \eta_2 \mathbf{I}_5 \end{aligned}$$

$$= \text{tr} \left[\hat{\eta}_1^T \left(\zeta_\eta \hat{\eta}_1 - \mathbf{I}_5 \mathbf{s}^T \right) \right] - \sum_{i=1}^5 K_i \frac{s_i^2}{\exp(s_i) + 1} \\ + \mathbf{s}^T \psi + \mathbf{s}^T \hat{\varepsilon} - \mathbf{s}^T \eta_1 \mathbf{I}_5 - \mathbf{s}^T \eta_2 \mathbf{I}_5 \quad (77)$$

Let us apply the update rule given by Eq. (58) in Eq. (77) to obtain

$$\dot{V} = \text{tr} \left[\hat{\eta}_1^T (\hat{\mathbf{s}}^* - \mathbf{s}^*) \right] - \sum_{i=1}^5 K_i \frac{s_i^2}{\exp(s_i) + 1} \\ + \mathbf{s}^T \psi + \mathbf{s}^T \hat{\varepsilon} - \mathbf{s}^T \eta_1 \mathbf{I}_5 - \mathbf{s}^T \eta_2 \mathbf{I}_5 \quad (78)$$

where $\hat{\mathbf{s}}^* = \text{diag} [\hat{s}_1, \dots, \hat{s}_5]$ and $\mathbf{s}^* = \text{diag} [s_1, \dots, s_5]$. Considering the convergence property of the state observer, Eq. (78) becomes

$$\dot{V} = - \sum_{i=1}^5 K_i \frac{s_i^2}{\exp(s_i) + 1} + \mathbf{s}^T \psi \\ + \mathbf{s}^T \hat{\varepsilon} - \mathbf{s}^T \eta_1 \mathbf{I}_5 - \mathbf{s}^T \eta_2 \mathbf{I}_5 \\ \leq - \sum_{i=1}^5 K_i \frac{s_i^2}{\exp(s_i) + 1} + \|\mathbf{s}\| (\|\psi\| - \|\eta_1\|) \\ + \|\mathbf{s}\| (\|\hat{\varepsilon}\| - \|\eta_2\|) \quad (79)$$

Considering that $\eta_2 = \text{diag} [\varrho |\hat{\varepsilon}_1|, \dots, \varrho |\hat{\varepsilon}_5|]$ with $\varrho \in \mathbb{R}^+$, we have $\|\eta_2\| = \varrho \|\hat{\varepsilon}\|$. Applying this late equality in Eq. (79), we obtain

$$\dot{V} \leq - \sum_{i=1}^5 K_i \frac{s_i^2}{\exp(s_i) + 1} + \|\mathbf{s}\| (\|\psi\| - \|\eta_1\|) \\ + \|\mathbf{s}\| \left(\frac{1}{\varrho} - 1 \right) \|\eta_2\| \quad (80)$$

Knowing that η_1 (which is not needed for the controller's implementation but that is used for stability analysis purpose only) is such as $\|\eta_1\| >> \|\psi\|$, and by selecting $\varrho > 1$, with $K_i \in \mathbb{R}^+$, we have $\dot{V} \leq 0$. This means that the closed-loop system is asymptotically stable regardless of the uncertain dynamics $\mathbf{f}(\mathbf{q}, \dot{\mathbf{q}})$, the disturbance torque, and the actuation fault (lumped disturbance $\psi(\dot{\mathbf{q}}, \tau)$). According to the Barbalat's lemma, $\mathbf{s} \rightarrow 0$, and therefore $\mathbf{e} \rightarrow 0$ as $t \rightarrow \infty$. Hence, we conclude that the control objective is achieved with the proposed control law used with the proposed dynamic parameters and update rules. This ends the proof of Theorem 1. \square

4 Simulation and discussion

In order to illustrate the efficiency of the proposed control algorithm for the 5-DOF upper-limb exoskeleton robot, in this section we present the results obtained when simulating the controlled system in MATLAB/SIMULINK. A benchmarking is performed by comparing these late results with those reported in [2].

For this simulation, the control objective is, as in [1] and [2], to force the links position vector \mathbf{q} to track the reference $\mathbf{q}_d = [q_{d,1}, \dots, q_{d,5}]^T$ where $q_{d,i} = 5 \sin(t + i\pi/5)$ for $1 \leq i \leq 5$.

For the high-gain state observer in Eq. (43) used to obtain an estimate state vector $\hat{\mathbf{x}}$, the high-gain matrix $\mathbf{L} = \text{diag} [L_1, \dots, L_5]$ is selected with $L_i^T = \begin{bmatrix} \frac{18}{\epsilon(t)} & \frac{9}{\epsilon(t)} \end{bmatrix}$ where $\epsilon(t)$ is obtained using Eq. (44). For the FNN used for approximating the system dynamics $\mathbf{f}(\mathbf{q}, \dot{\mathbf{q}})$, we use seven fuzzy rules for each link. For simplicity in the design, we use the same membership function for each link, given by

$$\mu_{A_l^j} = \exp \left[- \frac{(x_{ei,l} + 1.5 - (j-1)0.5)^2}{10^2} \right] \quad (81)$$

for $\mathbf{x}_{ei} = [\hat{q}_i, \dot{\hat{q}}_i]$, $i = 1, \dots, 5$, $j = 1, \dots, 7$ and $l = 1, 2$. The learning rate matrix for the FNN weight is selected as $\gamma = \text{diag} [\gamma_1, \dots, \gamma_5]$ where $\gamma_i = 1/15$ for $1 \leq i \leq 5$. For the controller's dynamic matrix parameter $\hat{\varepsilon}(t)$, the learning rate matrix is selected as $\zeta_\varepsilon = \text{diag} [\zeta_{\varepsilon,1}, \dots, \zeta_{\varepsilon,5}]$ with $\zeta_{\varepsilon,i} = 0.02$ for $1 \leq i \leq 5$. The learning rate matrix for the dynamic matrix $\hat{\eta}_1(t)$ is selected as $\zeta_\eta = \text{diag} [0.05 \ 0.05 \ 0.2 \ 0.5 \ 4]$. The sliding function uses a diagonal matrix $\Gamma \in \mathbb{R}^5$ for which all diagonal elements are equal to 15; we select $\varrho = 2$ for the parameter η_2 .

Remark 2 It is worth mentioning here that the choice of all the aforementioned constant design parameters may affect the tracking performances in terms of settling time and tracking accuracy. Their values are tuned during a trial-and-error process for which the outcome is a set of parameters that lead to optimal tracking performances. Just for illustration, the effect of the values selected for the controller's parameter $\mathbf{K} = \mathbf{K}^T \in \mathbb{R}^{5 \times 5}$ on the tracking performances can be observed by comparing results obtained for $K_i = 5$ and for

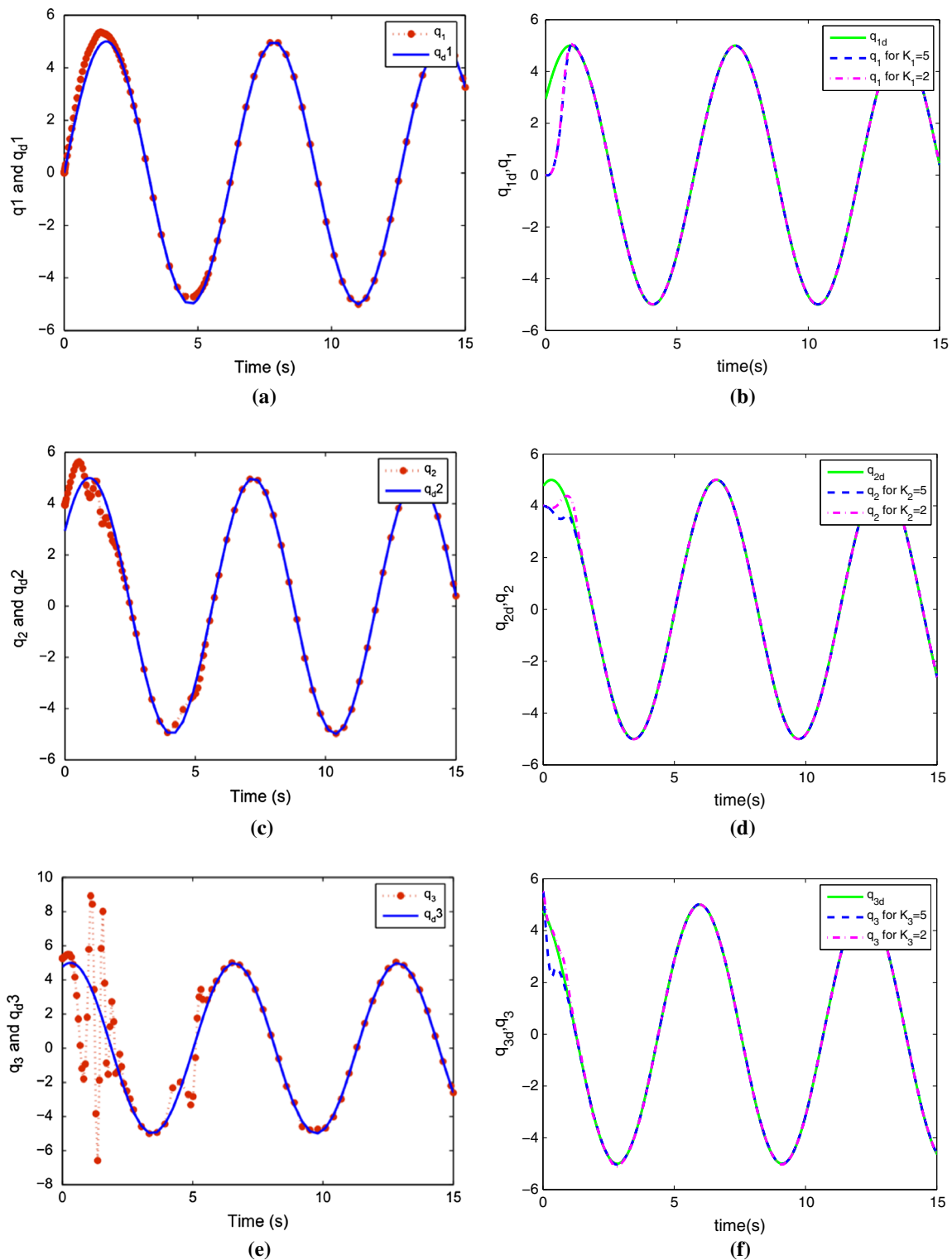


Fig. 1 Links' positions q_1, q_2 and q_3 for $K_1 = K_2 = K_3 = 5$ (dashed line) and for $K_1 = K_2 = K_3 = 2$ (dashdotted line) tracking the references q_{d1}, q_{d2} and q_{d3} with the nonlinear fault-

tolerant controller from [2] (see **a, c, e**), and with our nonlinear controller (see **b, d, f**)

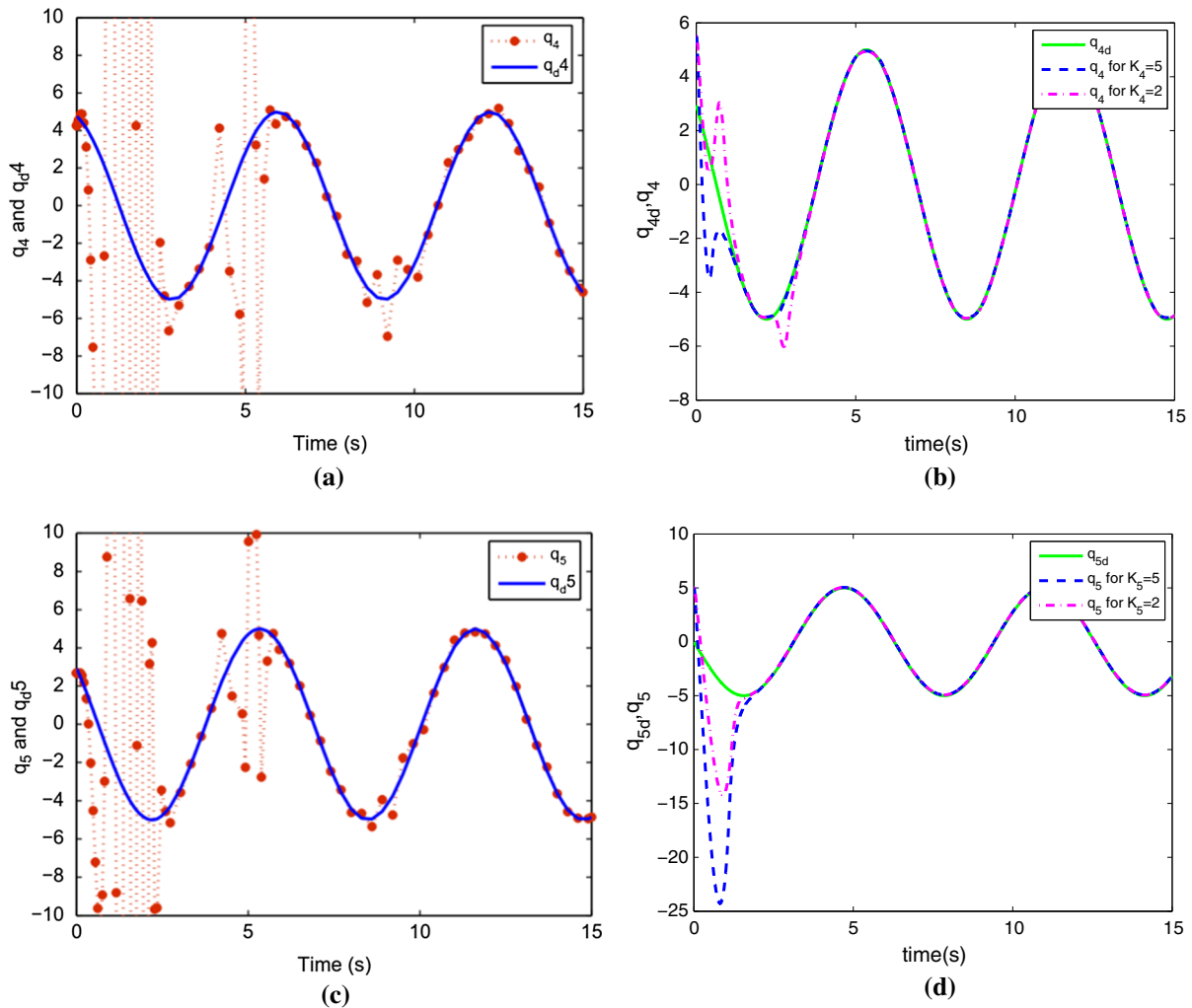


Fig. 2 Links' positions q_4 and q_5 for $K_4 = K_5 = 5$ (dashed line) and for $K_4 = K_5 = 2$ (dashdotted line) tracking the references q_{4d} and q_{5d} with the nonlinear fault-tolerant controller from [2] (see **a, c**), and with our nonlinear controller (see **b, d**)

$K_i = 2$ with $1 \leq i \leq 5$ (see dashed and dashdotted lines, respectively, on the right-hand side of Figs. 1, 2).

As in [2], for checking the performance of the control system when a torque disturbance and an actuation fault occur, we consider that at the time $t = 4s$, a disturbance torque $\tau_d = [\tau_{d1}, \dots, \tau_{d5}]$ with $\tau_{di} = 0.5 \text{ Nm}$ and a fault $\tau_a = 1.2\tau$ occur.

Figures 1 and 2 depict the 5-DOF upper-limb exoskeleton robot links positions q_1, \dots, q_5 tracking their references q_{d1}, \dots, q_{d5} when the FNN and observer-based nonlinear controller in Eq. (59) are used, and as reported in [2] where a fault-tolerant adap-

tive nonlinear controller was proposed for the same robotic system.

The plots on the left-hand-side of these figures represent the results reported in [2] while the ones on the right-hand-side are those obtained with the control law in Eq. (59). One can notice that the use of the control law in Eq. (59) leads to shorter settling time with fewer oscillations during the transient phase and better tracking accuracy. Information on the obtained approximate values of the minimum and maximum settling times on the five links with the two controllers can be found in Table 2.

Let us remind that only the robot's position information \mathbf{q} is available and that the controller uses the

Table 2 Some performance specifications on the five links with the controller Eq. (59) and the fault-tolerant adaptive nonlinear controller from [2]

Performance specifications	Equation (59)	Adapt. Nonl. contr. from [2]
Min settling time (s)	≈0.8	≈3
Max settling time (s)	≈2	≈6
$ \tau_i _{\max}$ in steady state (N m)	≈200	≈4900

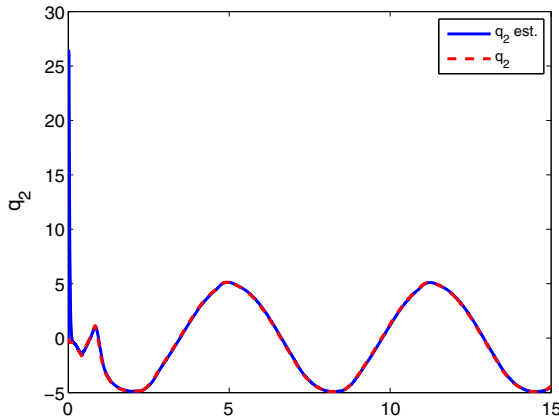


Fig. 3 Actual velocity \dot{q}_2 (dashed line) with its estimated value \hat{q}_2 for the 2nd link

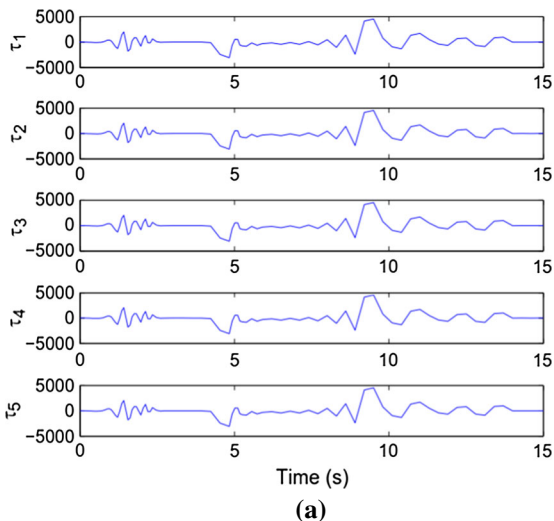
approximated position $\hat{\mathbf{q}}$ and velocity $\dot{\mathbf{q}}$ vectors. The good convergence ability of the employed high-gain observer is illustrated in Fig. 3 where the approximate velocity (continuous plot) for the robot's second link is represented along with its corresponding actual velocity (dashed plot).

Another important fact worth to be mentioned here is that the actuation effort needed to achieve the performance reported in [2] is away bigger than the one needed to achieve the improved performances obtained using the control law in Eq. (59). The control torques for the fives links obtained when the control law in Eq. (59) is applied, and the ones reported in [2] are portrayed in Fig. 4.

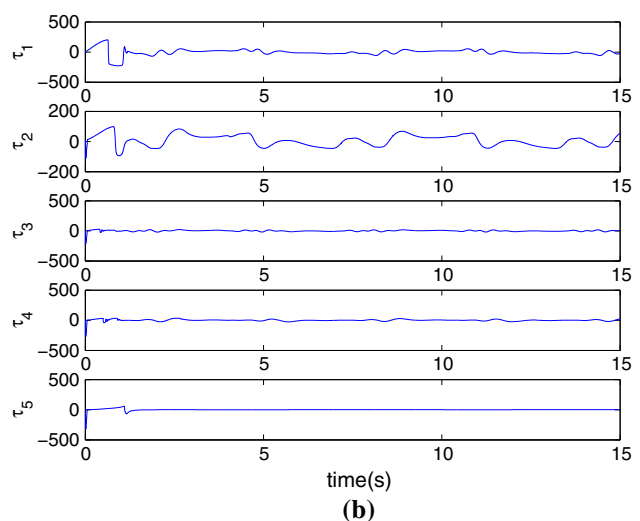
Table 2 provides an insight into the advantage of using the controller given by Eq. (59) by pointing out the fact that, with the control law reported in [2], considering each link individually, the maximum control effort in steady state is about 25 times bigger than when Eq. (59) is used for controlling the exoskeleton robot with unknowns dynamics, a disturbance torque and an actuation fault.

5 Conclusion

This paper has studied the design of a controller for a 5-DOF upper-limb exoskeleton robot used for pas-



(a)



(b)

Fig. 4 Five links actuation torques τ_1, \dots, τ_5 obtained: **a** with nonlinear fault-tolerant controller from [2]; **b** with the control approach proposed in this paper

sive rehabilitation therapy. The study has addressed challenges related to practical utilization of the robot such as uncertain nonlinear dynamics, unavailable full-state measurement, occurrence of disturbance torque, and actuation faults of different types. For tackling these challenges, an adaptive nonlinear control scheme, which is a new reaching law-based sliding mode control strategy, has been proposed. A high-gain state observer and a FNN have been used in the scheme for state vector and nonlinear dynamics estimation, respectively. Some dynamic parameters have been used in the scheme for efficiently and simultaneously tackling the effects of FNN approximation error, disturbance torque, and actuation faults. Simulation results have proved that fewer oscillations during transient phase, faster response, good tracking accuracy, and chattering-free control torques with lower amplitudes are obtained when the proposed scheme is employed. Future research will focus on extending the study presented in this work to propose an approach for the design of efficient observer-based adaptive fault-tolerant controllers for uncertain MIMO strict-feedback nonlinear systems with unknown control directions and constrained inputs.

References

- Kang, H.-B., Wang, J.-H.: Adaptive robust control of 5 DOF upper-limb exoskeleton robot. *Int. J. Control. Autom. Syst.* **13**(3), 733–741 (2015)
- Kang, H.-B., Wang, J.-H.: Adaptive control of 5 DOF upper-limb exoskeleton robot with improved safety. *ISA Trans.* **52**(3), 844–852 (2013)
- Ozkul, F., Barkana, D.E.: Design and control of an upper limb exoskeleton robot RehabRoby. In: TAROS 2011. LNAI 6856, pp. 125–136. Springer, Heidelberg (2011)
- Anam, K., Al-Jumaily, A.A.: Active exoskeleton control systems: state of the art. In: International Symposium on Robotics and Intelligent Sensors, vol. 41, pp. 107–123. Procedia Engineering (2012)
- Pons, J.L.: Wearable Robots: Biomechatronics Exoskeletons, vol. 70. Wiley, Hoboken (2008)
- Perry, J.C., Rosen, J., Burns, S.: Upper-limb powered exoskeleton design. *IEEE/ASME Trans. Mechatron.* **12**(4), 408–417 (2007)
- Hendricks, H.T., van Limbeek, J., Guerts, A.C., Zwarts, M.J.: Motor recovery after stroke: a systematic review. *Arch. Phys. Med. Rehabil.* **83**(11), 1629–1637 (2002)
- Nef, T., Nihelj, M., Riener, R.: ARMin: a robot for patient cooperative arm therapy. *Med. Biol. Eng. Comput.* **45**, 887–900 (2007)
- Khan, A.M., Yun, D.-W., Ali, M.A., Zuhaib, K.M., Yuan, C., Iqbal, J., Han, J., Shin, K., Han, C.: Passivity-based adaptive control for upper extremity assist exoskeleton. *Int. J. Control. Autom. Syst.* **14**(1), 291–300 (2016)
- Sandoval-Gonzalez, O., Jacinto-Villegas, J., Herrera-Aguilar, I., Portillo-Rodriguez, O., Tripicchio, P., Hernandez-Ramos, M., Flores-Cuaute, A., Avizzano, C.: Design and development of a hand exoskeleton robot for active and passive rehabilitation. *Int. J. Adv. Robot Syst.* (2016). doi:[10.5772/62404](https://doi.org/10.5772/62404)
- Tong, S., Wang, T., Li, Y.: Fuzzy adaptive actuator failure compensation control of uncertain stochastic nonlinear systems with unmodeled dynamics. *IEEE Trans. Fuzzy Syst.* **22**(3), 563–574 (2014)
- Li, Y., Tong, S., Li, T.: Adaptive fuzzy output-feedback control for output constrained nonlinear systems in the presence of input saturation. *Fuzzy Sets Syst.* **248**, 138–155 (2014)
- Tong, S., Min, C., Jun, Z.: Fuzzy adaptive output tracking control of nonlinear systems. In: 1999 IEEE International Fuzzy Systems Conference Proceedings. IEEE, Seoul (1999)
- Tong, S., Huo, B., Li, Y.: Observer-based adaptive decentralized fuzzy fault-tolerant control of nonlinear large-scale systems with actuator failures. *IEEE Trans. Fuzzy Syst.* **22**(1), 1–15 (2014)
- Li, Y., Tong, S.: Prescribed performance adaptive fuzzy output-feedback dynamic surface control for nonlinear large-scale systems with time delays. *Inf. Sci.* **292**, 125–142 (2015)
- Márton, L.: Actuator fault diagnosis in mechanical systems—fault power estimation approach. *Int. J. Control. Autom. Syst.* **13**(1), 110–119 (2015)
- Brambilla, D., Capisani, L.M., Ferrara, A., Pisù, P.: Fault detection for robot manipulators via second-order sliding modes. *IEEE Trans. Ind. Electron.* **55**(11), 3954–3963 (2008)
- Veluvolu, K.C., Defoort, M., Soh, Y.C.: High-gain observer with sliding mode for nonlinear state estimation and fault reconstruction. *J. Frankl. Inst.* **351**, 1995–2014 (2014)
- Veluvolu, K.C., Kim, M.Y., Lee, D.: Nonlinear sliding mode high-gain observers for fault estimation. *Int. J. Syst. Sci.* **42**, 1065–1074 (2011)
- Gholami, A., Markazi, A.H.D.: A new adaptive fuzzy sliding mode observer for a class of MIMO nonlinear systems. *Nonlinear Dyn.* **70**, 2095–2105 (2012)
- Goléa, N., Goléa, A., Barra, K., Bouktir, T.: Observer-based adaptive control of robot manipulators: fuzzy systems approach. *Appl. Soft Comput.* **8**, 778–787 (2008)
- Liu, Y.-J., Tong, S.-C., Wang, W., Li, Y.-M.: Observer-based direct adaptive fuzzy control of uncertain nonlinear systems and its applications. *Int. J. Control. Autom. Syst.* **7**(4), 681–690 (2009)
- Bugarian, A., Miranda, W., Forner-Cordero, A.: Upper limb exoskeleton control based on sliding mode control and feedback linearization. In: 2013 ISSNIP Biosignals and Biorobotics Conference (BRC), pp. 1–6. IEEE, Rio de Janeiro (2013)
- Wu, Q., Wang, X., Du, F., Zhu, Q.: Fuzzy sliding mode control of an upper limb exoskeleton for robot-assisted rehabilitation. In: 2015 International Symposium on Medical Measurements and Applications, pp. 451–456. IEEE, Turin (2015)

25. Liu, J., Wang, X.: Advanced Sliding Mode Control for Mechanical Systems. Tsinghua University Press, Beijing (2011)
26. Yin, C., Chen, Y., Zhong, S.: Fractional-order sliding mode based extremum seeking control of a class of nonlinear systems. *Automatica* **50**(12), 3173–3181 (2014)
27. Yin, C., Cheng, Y., Chen, Y., Stark, B., Zhong, S.: Adaptive fractional-order switching-type control method design for 3D fractional-order nonlinear systems. *Nonlinear Dyn.* **82**, 39–52 (2015)
28. Yin, C., Stark, B., Chen, Y., Zhong, S., Lau, E.: Fractional-order adaptive minimum energy cognitive lighting control strategy for the hybrid lighting system. *Energy Build.* **87**, 176–184 (2015)
29. Zhao, X., Shi, P., Zheng, X., Zhang, L.: Adaptive tracking control for switched stochastic nonlinear systems with unknown actuator dead-zone. *Automatica* **60**, 193–200 (2015)
30. Zhao, X., Shi, P., Zheng, X., Zhang, J.: Intelligent tracking control for a class of uncertain high-order nonlinear systems. *IEEE Trans. Neural Netw. Learn. Syst.* (2015). doi:[10.1109/TNNLS.2015.2460236](https://doi.org/10.1109/TNNLS.2015.2460236)
31. Rahman, M.H., Saad, M., Kenné, J.P., Archambault, P.S.: Exoskeleton robot for rehabilitation of elbow and forearm movements. In: 18th Mediterranean Conference on Control and Automation Congress. IEEE, Marrakech (2010)
32. Rahman, M.H., Archambault, P.S., Saad, M., Luna, C.O., Ferrer, S.B.: Robot aided passive rehabilitation using nonlinear control techniques. In: 9th Asian Control Conference (ASCC). IEEE, Istanbul (2013)
33. Babaieasl, M., Goldar, S.N., Barhaghtalab, M.H., Meigoli, V.: Sliding mode control of an exoskeleton robot for use in upper-limb rehabilitation. In: Proceedings of the 3rd RSI International Conference on Robotics and Mechatronics. IEEE, Tehran (2015)
34. Soltanpour, M.R., Khooban, M.H.: A particle swarm optimization approach for fuzzy sliding mode control for tracking the robot manipulator. *Nonlinear Dyn.* **74**, 467–478 (2013)
35. Ju, M.-S., Lin, C.-C.K., Lin, D.-H., Hwang, I.-S., Chen, S.-M.: A rehabilitation robot with force-position hybrid fuzzy controller: hybrid fuzzy control of rehabilitation robot. *IEEE Trans. Neural Syst. Rehabil. Eng.* **13**(3), 349–358 (2005)
36. Denève, A., Moughamir, S., Afifal, L., Zayton, J.: Control system design of a 3-DOF upper limb rehabilitation robot. *Comput. Methods Programs Biomed.* **89**, 202–214 (2008)
37. Komada, S., Hashimoto, Y., Okuyama, N., Hisada, T., Hirai, J.: Development of a biofeedback therapeutic-exercise-supporting manipulator. *IEEE Trans. Ind. Electron.* **56**(10), 3914–3920 (2009)
38. Dombre, E.: Analyse et modélisation des robots manipulateurs. Hermès Publications, Paris (2001)
39. Rahman, M.H., Saad, M., Kenné, J.P., Archambault, P.S.: Nonlinear sliding mode control implementation of an upper limb exoskeleton robot to provide passive rehabilitation therapy. In: ICIRA 2012. Part II, LNAI 7507, pp. 52–62. Springer, Berlin (2012)
40. Rahman, M.H., Saad, M., Kenné, J.P., Archambault, P.S.: Control of an exoskeleton robot arm with sliding mode exponential reaching law. *Int. J. Control. Autom. Syst.* **11**(1), 92–104 (2013)
41. Xin, M., Fei, J.: An adaptive fuzzy sliding mode controller for MEMS triaxial gyroscope with angular velocity estimation. *Nonlinear Dyn.* (2012). doi:[10.1007/s11071-012-0433-z](https://doi.org/10.1007/s11071-012-0433-z)
42. Du, H., Yu, X., Chen, M.Z.Q., Li, S.: Chattering-free discrete-time sliding mode control. *Automatica* **68**(6), 81–91 (2016)
43. Khalil, H.K.: Nonlinear Systems, 3rd edn. Prentice Hall, Upper Saddle River (2002)
44. Fallaha, C.J., Saad, M., Kanaan, H.Y., Al-Haddad, K.: Sliding-mode robot control with exponential reaching law. *IEEE Trans. Ind. Electron.* **58**(2), 600–610 (2011)
45. De Luca, A., Mattone, R.: An identification scheme for robot actuator faults. In: 2005 IEEE/RSJ International Conference on Intelligent Robots and Systems, pp. 1127–1131. IEEE (2005)
46. Caccavale, F., Cilibrizzi, P., Villani, L.: Actuators fault diagnosis for robot manipulators with uncertain model. *Control Eng. Pract.* **17**(1), 146–157 (2009)
47. Asada, H., Youcef-Toumi, K.: Analysis and design of a direct-drive arm with five-bar-link parallel drive mechanism. *ASME J. Dyn. Syst. Meas. Control* **106**(3), 225–230 (1984)
48. Perruquetti, W., Barbot, J.P.: Sliding Mode Control in Engineering. Marcel Dekker, Inc., New York (2002)
49. Slotine, J.J.E., Li, W.: Applied Nonlinear Control. Prentice-Hall, Engelwood Cliffs (1991)
50. Aschmann, H., Schindeler, D.: Sliding-mode control of a high-speed linear axis driven by pneumatic muscle actuators. *IEEE Trans. Ind. Electron.* **55**(11), 3855–3864 (2008)
51. Orlowska-Kowalska, T., Kaminski, M., Szabat, K.: Implementation of a sliding-mode controller with an integral function and fuzzy gain value for electrical drive with an elastic joint. *IEEE Trans. Ind. Electron.* **57**(4), 1309–1317 (2010)
52. Kawamura, A., Ito, H., Sakamoto, K.: Chattering reduction of disturbance observer based sliding mode control. *IEEE Trans. Ind. Appl.* **30**(2), 456–461 (1994)
53. Tai, N., Ahn, K.: A RBF neural network sliding mode controller for SMA actuator. *Int. J. Control. Autom. Syst.* **8**(6), 1296–1305 (2010)
54. Gao, W.B., Hung, J.C.: Variable structure control of nonlinear-systems—a new approach. *IEEE Trans. Ind. Electron.* **40**(1), 45–55 (1993)
55. Rong, H.-J.: Indirect adaptive fuzzy-neural control of robot manipulator. In: 2012 IEEE 9th International Conference on High Performance Computing and Communications and 2012 IEEE 14th International Conference on Embedded Software and Systems (HPCC-ICESS). IEEE, Liverpool (2012)
56. Kiguchi, K., Hayashi, Y.: An EMG-based control for an upper-limb power-assist exoskeleton robot. *IEEE Trans. Syst. Man Cybern. Part B Cybern.* **42**(4), 1064–1071 (2012)
57. Gunasekara, J.M.P., Gopura, R.A.R.C., Jayawardane, T.S.S., Lalitharathne, S.W.H.M.T.D.: Control methodologies for upper limb exoskeleton robots. In: 2012 IEEE/SICE International Symposium on System Integration (SII). IEEE, Fukuoka (2012)
58. Pratap, B., Purwar, S.: Sliding mode state observer for 2-DOF twin rotor MIMO system. In: 2010 International Conference on Power, Control and Embedded Systems (ICPCES), pp. 1–6. IEEE, Allahabad (2010)

59. Veluvolu, K.C., Zhe, F., Soh, Y.C.: Nonlinear sliding mode high-gain observers for fault detection. In: 2010 International Workshop on Variable Structure Systems, pp. 203–208. IEEE, Mexico City (2010)
60. Veluvolu, K.C., Soh, Y.C., Cao, W.: Robust observer with sliding mode estimation for nonlinear uncertain systems. IET Control Theory Appl. **1**(5), 1533–1540 (2007)
61. Fuller, R.: Neural Fuzzy Systems. Abo Akademi University, Abo (1995)
62. Mushage, B.O., Chedjou, J.C., Kyamakya, K.: An extended neuro-fuzzy-based robust adaptive sliding mode controller for linearizable systems and its applications on a new chaotic system. Nonlinear Dyn. **83**, 1601–1619 (2016)

Reproduced with permission of copyright owner. Further reproduction
prohibited without permission.